THE STRUCTURE AND FLAME PROPAGATION REGIMES IN TURBULENT HYDROGEN JETS

A. Veser[1], M. Kuznetsov[2], G. Fast[2], A. Friedrich[1], N. Kotchourko[1], G. Stern[1], M. Schwall[2], W. Breitung[2]
[1] ProScience GmbH, Parkstr. 9, 76275 Ettlingen, Germany
[2] Research Center Karlsruhe, P.O. Box 3640, 76021 Karlsruhe, Germany

Corresponding author: kuznetsov@iket.fzk.de

ABSTRACT

Experiments on flame propagation regimes in a turbulent hydrogen jet with velocity and hydrogen concentration gradients have been performed at the FZK hydrogen test site HYKA. Horizontal stationary hydrogen jets released at normal and cryogenic temperatures of 290K and 80 and 35K with different nozzle diameters and mass flow rates in the range from 0.3 to 6.5 g/s have been investigated. Sampling probe method and laser PIV technique have been used to evaluate distribution of hydrogen concentration and flow velocity along and across the jet axis. High-speed photography (1000 fps) combined with a Background Oriented Schlieren (BOS) system was used for the visual observation of the turbulent flame propagation. In order to investigate different flame propagation regimes the ignition position was changed along the jet axis. It was found that the maximum flame velocity and pressure loads can only occur if the hydrogen concentration at the ignition point exceeds 11% of hydrogen in air. In this case the flame propagates in both directions, up- and downstream the jet flow, whereas in the opposite case, the flame propagates only downstream. Such a behavior is consistent with previous experiments, according to that the flame is able to accelerate effectively only if the expansion rate σ of the H_2-air mixture is higher than a critical value $\sigma^* = 3.75$ (like for the 11% hydrogen-air mixture). The measured data allow conservative estimates of the safety distance and risk assessment for realistic hydrogen leaks.

1.0 INTRODUCTION

Recently the hydrogen economy develops intensively as an alternative to the oil industry and on behalf of the solution of the global warming problem. One of the promising ideas is to use hydrogen as an energy carrier and a fuel simultaneously. The idea could be realized using a cable system which integrates an electric power supply and a pressurized liquid hydrogen (LH_2) pipeline in order to deliver energy and fuel to a customer [1]. In the current work we consider an accident scenario in which the hydrogen pipeline is broken and the released hydrogen jet is ignited. In order to estimate the hazard potential we have initially studied the properties of unburned and burned hydrogen jets released from a pressurized pipeline at ambient temperature of about 293K to compare the same properties for a hydrogen jet at cryogenic temperature of (80K and 35K). The flow velocity, hydrogen distribution and scaling characteristics for a high momentum hydrogen jet have been intensively investigated at the Sandia National Laboratory (SNL) [2]. Experimental data of the SNL performed for hydrogen jets with an initial pressure of up to 70 bar are consistent with the well known correlations [3] obtained for axial concentrations C(x)

$$C(x) = A \cdot C_0 \cdot \frac{d_{ef}}{x} \left(\frac{\rho_a}{\rho_{H_2}} \right)^{1/2}, \qquad (1)$$

and the axial flow velocity u(x) as function of distance from the nozzle in the high momentum jet:

$$u(x) = u_0 \cdot B \cdot \left(\frac{x - x_0}{d_0} \right)^{-1}, \qquad (2)$$

where A and B are empirical constants; C_0 and u_0 are initial hydrogen concentration and flow velocity; d_0 is the nozzle diameter; ρ_a and ρ_{H2} are densities of ambient air and hydrogen; d_{ef} is an effective nozzle diameter calculated as follows [3]

$$d_{ef} = d_0 \sqrt{C_D \frac{p}{p_a} \left(\frac{2}{\gamma + 1} \right)^{\frac{\gamma+1}{2(\gamma-1)}}}, \tag{3}$$

where C_D is a discharge coefficient; p and p_a are internal and ambient pressures; $\gamma = c_p/c_v$ is specific heats ratio. For each cross-section $x = x_i$ of the high momentum jet (Fig. 1), the hydrogen concentration and flow velocity have normal distribution across the flow which is described well by a Gauss function:

$$C_{H_2}(r) = \frac{A_0}{\sigma\sqrt{2\pi}} \exp\left(-\frac{(r-\mu)^2}{2\sigma^2} \right)^{1/2}, \tag{4}$$

$$u(r) = \frac{B_0}{\sigma\sqrt{2\pi}} \exp\left(-\frac{(r-\mu)^2}{2\sigma^2} \right)^{1/2}, \tag{5}$$

where r is the distance from the jet axis; $A_0/(\sigma\cdot(2\pi)^{1/2}) = C(x)$ and $B_0/(\sigma\cdot(2\pi)^{1/2}) = u(x)$ are the maximum local hydrogen concentration and flow velocity on the jet axis. Knowing all parameters of the equations (1)-(5) we can predict hydrogen concentration and flow velocity fields in the jet in order to evaluate flammability of the jet and possible flame propagation regime. Figure 1 schematically shows the burnable zone of a stationary hydrogen jet as a region with hydrogen concentrations within the hydrogen flammability limits in air (4-75 Vol. $\%H_2$).

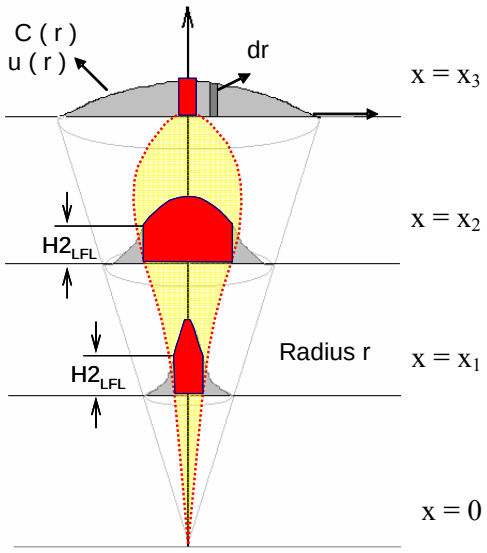

Figure 1. Hydrogen distribution in free hydrogen jet: $H2_{LFL}$ is the lower flammability limit

Theoretically, amount of burnable hydrogen within the flammability limits in case of "late" ignition of stationary hydrogen jet can be evaluated. This estimation will be based on the existing flammability limits obtained for stagnant hydrogen-air mixtures and on the assumption of complete hydrogen combustion. It gives a very conservative value for the mass of burned hydrogen in a jet. It does not take into account any effects of the highly turbulent flow on the combustion in a free hydrogen jet.

Depending on the mixture sensitivity, the turbulence in the jet can promote or suppress flame propagation with following flame acceleration or, in opposite case, it can lead to a local quenching of an initially ignited mixture. As it was found in [4] the expansion ratio σ, which is equal to density ratios of unburnt and burnt gas, can characterize the potential for effective flame acceleration in presence of well developed turbulence generated by obstacles, fans, grids, etc. A critical expansion ratio of $\sigma^* = 3.75$ was found for an effective flame acceleration for hydrogen-air mixtures at NTP [4]. This critical expansion ratio corresponds to a hydrogen-air mixture with ~11% of hydrogen and more reactive mixtures (>11%H_2) with a higher expansion ratio ($\sigma > \sigma^*$) can effectively accelerate sonic speed in a highly turbulent flow. If the mixture would be less reactive than the critical one (<11%H_2) the turbulence will lead to a flame deceleration or local quenching. Applying this theory to the free turbulent hydrogen jet we can expect that the turbulence will suppress flame propagation and reduce the size of the combustible zone for the mixtures between the flammability limit (4%H_2) and flame acceleration (FA) limit (11%H_2).

All data on flame acceleration in turbulent flows in [4] have been obtained for uniform premixed gas compositions in obstructed channels. In a free hydrogen jet we have an open gas system with highly nonuniform distribution of hydrogen concentrations and flow velocities along and across the jet. The main purpose of the current work is to investigate the flame propagation regimes in the free turbulent hydrogen jet in presence of nonuniform flow velocity and hydrogen distribution.

2.0 EXPERIMENTAL DETAILS

2.1 Hydrogen Injection System

For the experimental investigation of the hydrogen distribution in a horizontal jet and the hydrogen combustion following an ignition, a facility was constructed at the HYKA test site of the Institute for Nuclear and Energy Technologies of the FZK. The hydrogen is taken from gas cylinders and regulated in pressure, temperature and mass flow through a bypass configuration. The hydrogen jet is then generated by simultaneously closing the bypass valve and opening the main valve with an effective inner diameter of 10 mm each. In both cases the hydrogen is released into an attached 60 mm long pipe with an inner diameter of 10 mm, see Fig. 2, which feeds a defined orifice (Ø1, 2 or 4 mm). The design is identical in construction for both, the bypass and the main pathway, where the jet enters the ambient air. The fast-acting pneumatic valves are synchronized to provide the control variables during the generation of the horizontal jet.

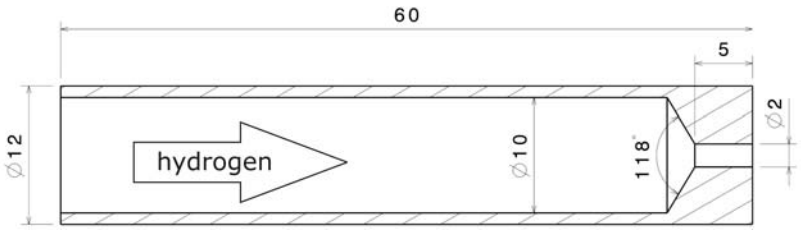

Figure 2. Sketch of the pipe section with orifice on the right hand side (all dimensions in mm)

The inner dimensions of the experimental test chamber are 5.5 x 8.5 x 3.4 m and are large enough compared to the jet region. The orifice is positioned 0.9 m above the ground to avoid wall effects. The horizontal orientation of the orifice is adjusted by laser alignment.

The initial pressure of the released hydrogen is changed in the range 5-60 bar for different experiments. Experiments have been performed at ambient and cryogenic temperatures 290-298K and 80K. Pressure and temperature of the pressurized hydrogen are measured within the pipe section - centrally between the valve and the orifice. The temperature is recorded by type K thermocouples with

a measurement uncertainty of ± 2K. The pressure sensors have a maximum error of ± 0.5%. The hydrogen mass flow is limited to sound speed in the orifice because in all working points the fluid-dynamic critical pressure ratio is exceeded. Thus, the hydrogen discharge through the orifice causes an under-expanded jet.

2.2 Measurements and Experimental Data Acquisition

The facility is equipped with different measurement systems. For cold jet and flame visualization the Background Oriented Schlieren (BOS) technique is applied. Another non-intrusive optical method is the Particle Image Velocimetry (PIV) for the determination of the 2D jet velocity field. Hydrogen concentrations are measured with gas probes. All measurement systems are synchronized with the injection control, so that the hydrogen jet possesses a high temporal reproducibility. The Background Oriented Schlieren (BOS) technique described in [5] is based on the optical deformation of a background pattern due to density gradients in the gas system under investigation. The method is similar to the schlieren technique and very effective for gases with a density difference like hydrogen jet in air and for investigation of combustion processes. The method uses digital CCD camera recording followed by digital image processing.

The hydrogen jet velocity is measured with PIV in a 2D velocity field as $\vec{v} = (u, v)$. This technique uses tracer particles with a mean diameter below 2 µm that are seeded into the hydrogen jet in order to provide sufficient flow tracking ability [6]. These particles are sucked into the hydrogen jet together with the entrainment air. A fast double-frame camera captures the Mie scattering signals that arise by the illumination within a laser light sheet from two laser shots. The time delay between the two shots is adjusted to allow an optimum traveling displacement of the particles in the images. Depending on the local velocities typical time delays range between 1 µs and 12 µs. The PIV lasers are installed together with the camera and the optical bench on a sliding carriage that is traversed along the jet axis.

Supplementary information is gained by direct measurements of local hydrogen concentration within the jet. The gas probes consist of cylinders of 0.3 dm^3 volume which are evacuated before the experiment. Synchronized valves control the time of inflow and measurement duration. The cylinder content is analyzed off-line after the experiment with an uncertainty of ± 0.1%. The probes are positioned at different locations within the jet. Fig. 3 shows an example of hydrogen distribution obtained using the sampling probe method in two different cross-sections. The hydrogen distribution profile is ideally described as Gauss function according to equations (4-5).

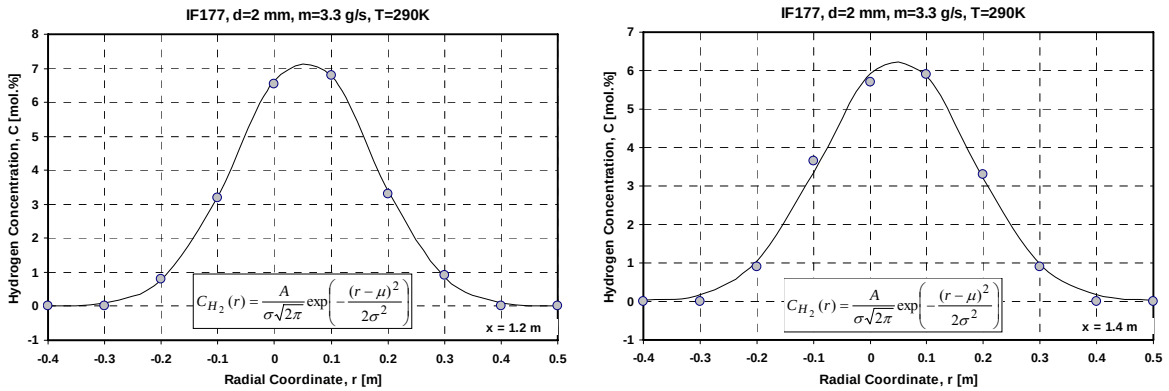

Figure 3. Measured radial hydrogen distribution in a jet at distances x = 1.2 and 1.4 m from the nozzle

3.0 EXPERIMENTAL RESULTS

3.1 Hydrogen Jet Structure

Two experimental series have been performed. The first one concerns the hydrogen jet itself, without combustion, in order to investigate hydrogen concentration and flow velocity distribution in the jet. Fig. 4 depicts a schlieren image of the horizontal hydrogen jet. The BOS image shows axisymmetric spreading of the mixture of hydrogen and entrained air for the major jet part downstream the orifice. Up to a distance of ~2 m from the nozzle, the jet shows no visible influence of buoyancy effects. Hydrogen distribution proceeds in a buoyant cloud at the end of the jet. Thus the jet behaves as a typical high-momentum jet in this example. The charging time of the injection tube is very short, so that the macroscopic characteristics of the hydrogen jet reach practically steady-state conditions early in the release experiments.

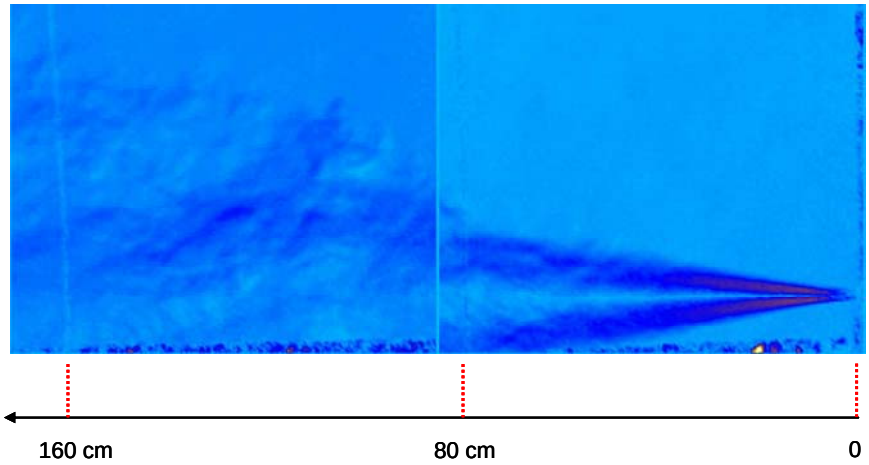

Figure 4. BOS image of horizontal jet (nozzle Ø4 mm, p = 10 bar)

As Fig. 5 indicates, all tested hydrogen jets at different initial pressures and nozzle diameters satisfy the conditions for high-momentum jets according to densimetric Froude number (Fr > 1000). This means that the horizontal jet has an axial symmetry and all dependencies and correlations (1-5) obtained for vertical jets can also be used.

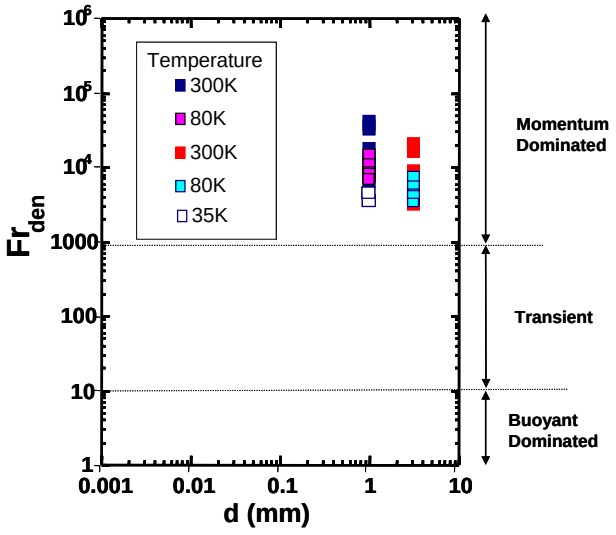

Figure 5. Froude number diagram for different strength of hydrogen jet (points = current experiments)

The Particle Image Velocimetry method was used to obtain radial flow velocities at different distances from the nozzle. In each axial position 100 image pairs of the particle-seeded hydrogen jet were recorded from which instantaneous velocity fields and ensemble averaged velocities were calculated. As an example, the experimental results for radial velocity profiles of hydrogen at 1.92 MPa and 290 K in the injection tube that expands to ambient air are presented here (Fig. 6). The jet conditions correspond to a densimetric Froude number of 13000 which indicates the highly inertia dominated flow. The opening of the circular orifice is d_0 = 2 mm as shown in Fig. 2. The associated measured hydrogen mass flow is 3.3 g/s with a measurement uncertainty of ± 0.35%. The spatial evolution of the mean radial velocity profile along the jet axis is shown for different positions x/d_0 in Fig. 6. The velocity scale given at the top corresponds to the velocity profile for x/d_0 = 25. For other x/d_0 values this velocity scale has to be shifted, e.g. to x/d_0 = 100 for the red triangles. The measured radial velocity profiles at different distances from the nozzle have a typical Gaussian profile which can be described by equation (5). In the shear layer the velocity profile broadens in downstream direction due to the entrainment and acceleration of surrounding air. The radii of the half maximum velocity $r_{0.5u}$ at the center line are marked with open circles. The spreading rate $dr_{0.5u}/dx$ has a constant value of 0.09. This validates the similarity region of the jet and is in good agreement to other experiments [2].

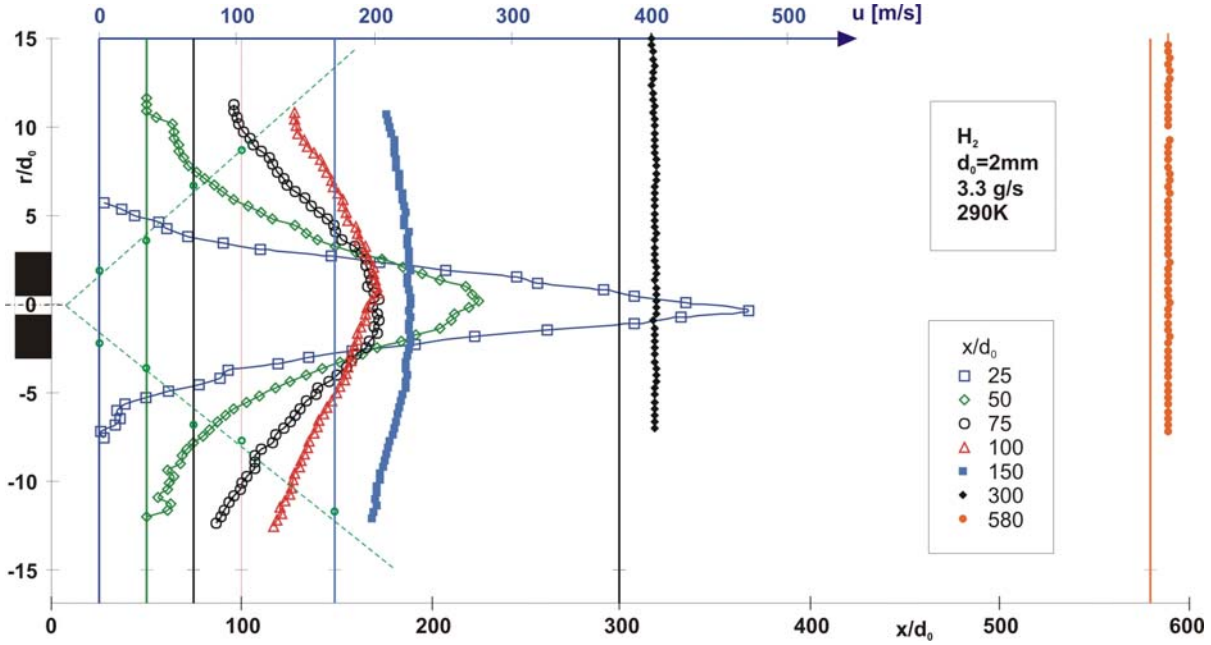

Figure 6. PIV results for radial velocity profiles as function of distance from the nozzle

The mean axial velocity of the underexpanded hydrogen jet decays rapidly with increasing distance from the nozzle. Fig. 7 presents the mean measured axial velocities and its reciprocal values along the jet centerline. The hyperbolic decay of the mean center line velocity is revealed at nozzle distances $x/d_0 > 25$. Upstream of this distance typical shock diamonds are found in the BOS images. These supersonic flow structures prevent a sufficient entrainment of the aerosol tracer and therefore cross-correlation of PIV data is not possible. The hyperbolic decrease in the measured velocity indicates that the acceleration of the tracer particles to the velocity of their carrier fluid is completed at this distance. The flow velocity in a jet can be scaled with the sound speed and equivalent nozzle diameter which includes a ratio of the initial hydrogen density to the ambient air density. The sound speed is reached at the orifice cross section. With an excellent agreement at short distances, the velocity decay is described by [3]:

$$u_a = u_0 \; B \left(\frac{x - x_0}{d_0} \right)^{-1}, \tag{6}$$

with the sound speed $u_0 = 1283$ m/s, the virtual jet origin $x_0 = 19\ d_0$ and the slope B = 5.8. Taking into account the root of the density ratio before and after the orifice $(\rho_0/\rho_\infty)^{1/2} = 1.14$, the equivalent slope becomes $B_e = 5.1$. Both values of B lie between 5 and 6 as stated by Chen&Rodi [3]. Subsonic jets normally show negative values for the virtual jet origin. The positive and high value of x_0 can be attributed to the dimension of the Mach disc and jet expansion to 1 bar. Therefore the underexpanded jet shows subsonic jet characteristics from a downstream shifted virtual origin.

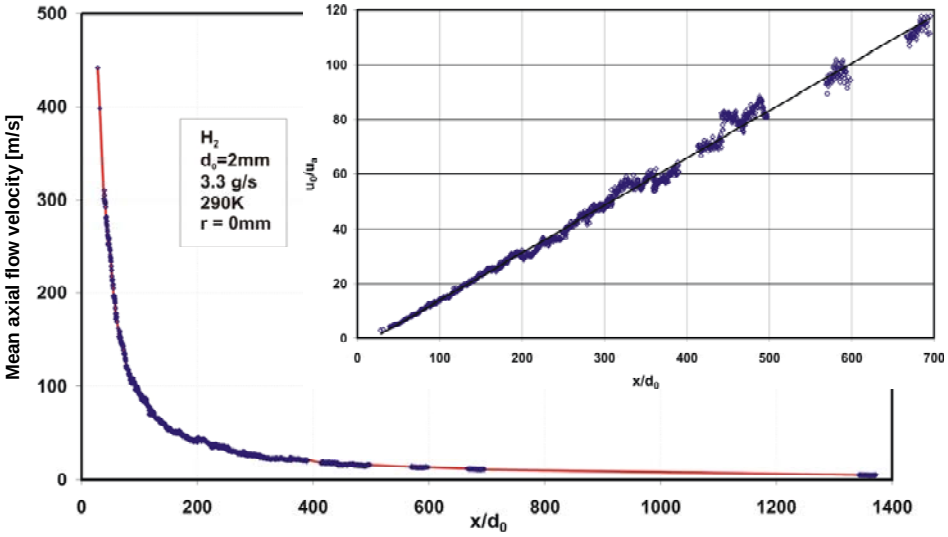

Figure 7. Measured mean axial velocity as function of distance from the nozzle: subpicture is in reciprocal velocity scale, normalized by the sound speed of hydrogen

With the PIV method the major turbulence energy of the large-scale turbulence is detected by ensemble statistics of local velocities. The detected turbulence frequency is limited by the PIV time step between the image pairs as stated above. The measured mean axial velocity fluctuations $u_{rms}/\bar{u}$ at the center line are already 30% at a distance of 25 d_0 (Fig. 8). This turbulence level remains the same for all measured positions along the jet axis. The averaged radial turbulence level $v_{rms}/\bar{v}$ increases from 22% at 25 d_0 to 30% at 1400 d_0.

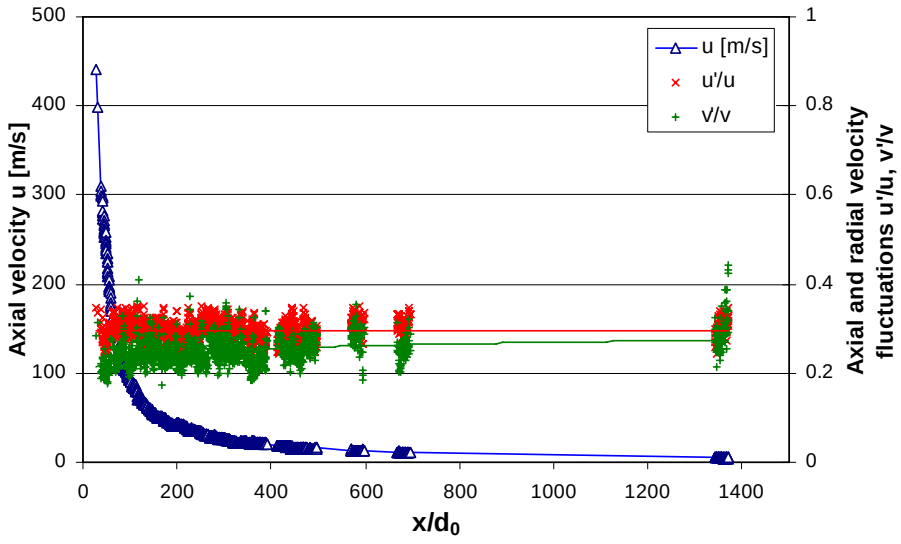

Figure 8. Axial and radial velocity fluctuations in a hydrogen jet

Hydrogen concentration measurements were performed under the same nominal conditions as the velocity measurements with only small deviations. As it follows from Fig. 3, the radial hydrogen concentration in a jet has typical Gaussian profile similar to the radial velocity distribution (Fig. 6). The axial hydrogen concentrations also decay with increasing distance from the nozzle. In Fig. 9 the reciprocal value of the measured axial hydrogen concentration is shown as a dependence against normalized nozzle distance x/d_0. The measurements at different pressures and temperatures with two different nozzle diameters d_0 collapse into one single relation except the temperature of 35K. The linearity of the dependency demonstrates the hyperbolical decay of the concentration at the center line. Thus, the hydrogen jet with an air entrainment can be described by similarity laws within the horizontal jet region according to Eq. 1. Different behavior of the hydrogen jet at the lowest temperature of 35K can be explained by the two phase flow effect.

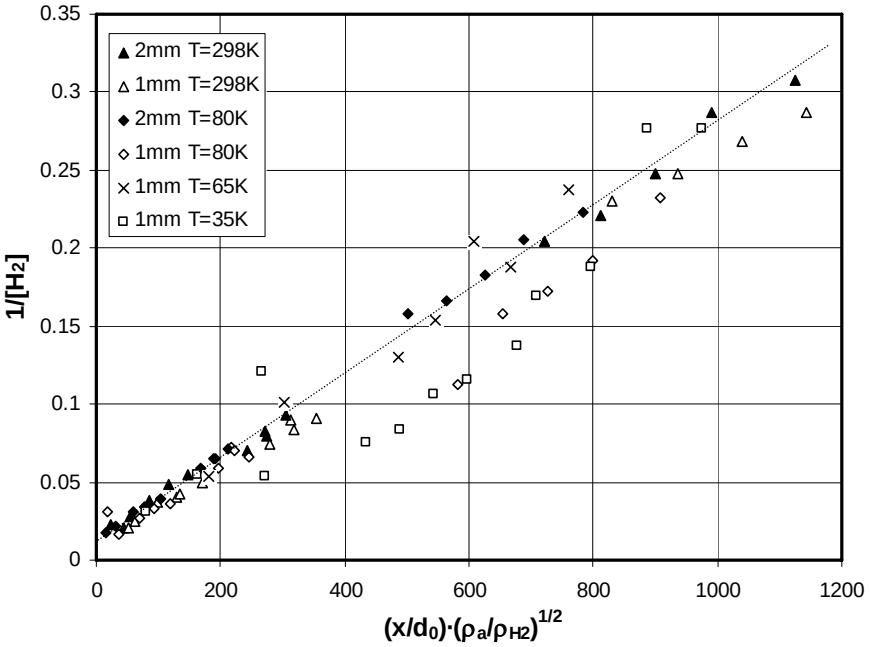

Figure 9. Measured reciprocal hydrogen concentration vs. normalized distance from the nozzle for two different nozzle diameters d_0

3.2 Ignition Experiments

The previous experiments demonstrated the highly nonuniform distribution of flow velocity and hydrogen concentration in the horizontal high momentum jets. It can be regarded as a gas system with axial and radial reactivity gradients in the presence of a well developed turbulent flow. A scenario with "late" ignition of hydrogen jet will be considered here. In such case the ignition of well established steady-state hydrogen jet takes place. The results of an ignition process and the following flame propagation will depend on the location of the ignition point. Investigation of flame propagation regimes for different ignition point locations have been performed in the second part of this work. The distance from the ignition point to the nozzle was changed in the range 50–275 cm. Fig. 10 demonstrates two typical flame propagation regimes depending on the ignition distance. The first regime is a "fast" combustion, where after ignition the flame propagates in both directions: up- and downstream. The flame is stabilized near the nozzle and does not depend on the later ignition source operations. The visible downstream flame velocity close to the ignition point was measured to be 50–70 m/s. Then the velocity decays to 20–25 m/s at the distance 0.5-0.8 m from ignition point. The maximum upstream flame velocity in the laboratory frame (against the jet velocity) reaches 18 m/s at a distance 30 cm from the ignition point. The second observed combustion regime is a "slow" unstable combustion in which the flame propagates only downstream. The combustible zone is stabilized by the

active ignition source as long as it is operating. After the spark generator is turned off the flame immediately moves downstream and than quenches.

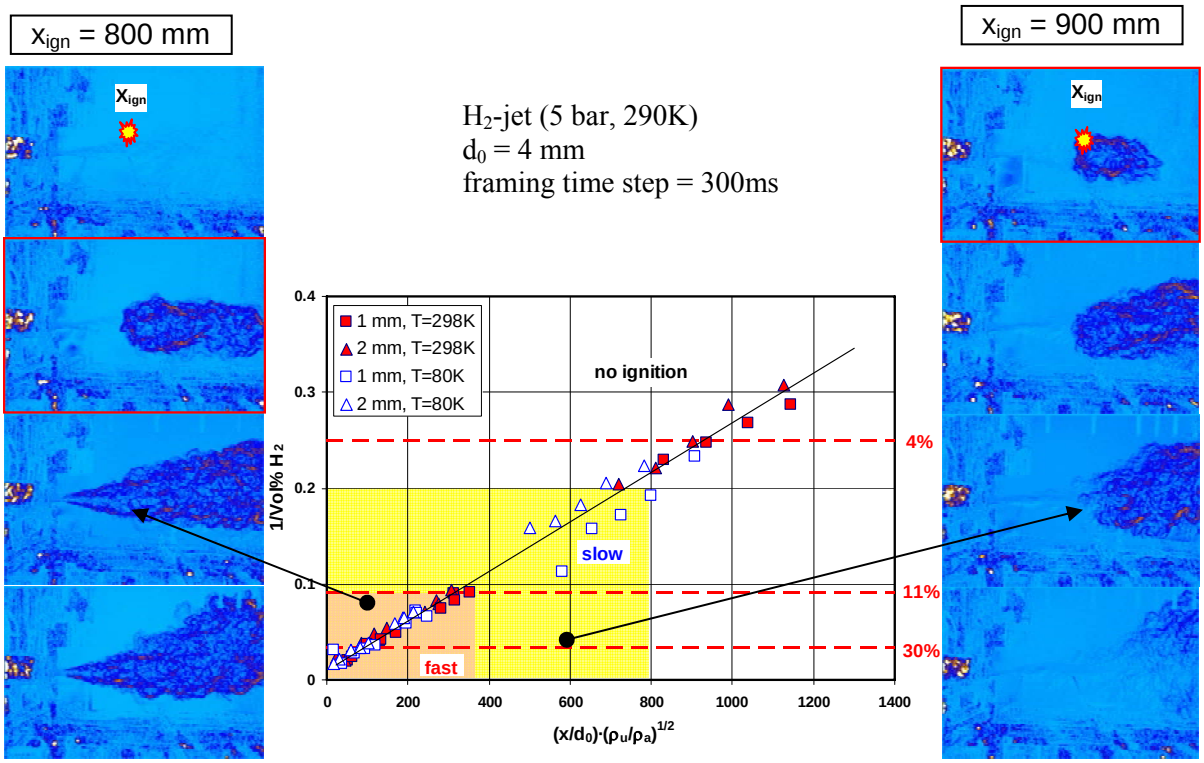

Figure 10. BOS images of two combustion regimes with a state diagram for combustion regimes

With known axial hydrogen concentration and flow velocity dependencies we found that the threshold between the two flame propagation regimes corresponds to the distance from the nozzle where the hydrogen concentration is equal to 11% H_2. This value is in excellent consistency with experimental data on critical conditions for effective flame acceleration in an obstructed channel [4]. Using the expansion ratio σ as a criterion for effective flame acceleration it was found that the critical expansion ratio is $\sigma^* = 3.75$ for hydrogen – air mixtures under normal initial conditions. This value $\sigma^* = 3.75$ exactly corresponds to the hydrogen-air mixture with 11% H_2.

Fig. 11 is based on the previously described experimental data for jet characteristics. It shows hydrogen concentration (11%) and flow velocity (u = 57 m/s) corresponding to the threshold between "fast" and "slow" flame propagation in the jet. The flow velocity at the ignition point is very close to the measured flame velocity (u = 50-70 m/s). With decreasing flow velocity and mixture reactivity of the jet the visible downstream flame velocity also decreases. The flame behavior in the opposite direction is not so evident but using the Borghi state diagram of turbulent combustion regimes the flame behavior upstream the flow can be estimated. Assuming the flow velocity u = 57 m/s at the critical ignition point and the turbulent velocity fluctuations u'/u =25% (see Fig. 8) a value of $u'/S_L \sim 70$ is obtained for a 11% H2-air mixture with a laminar flame speed of $S_L = 0.2$ m/s. On the other hand, with an average characteristic integral scale of turbulent vortices in the jet of the order l_T = 5 cm (size of eddies at critical point) and laminar flame thickness $\delta_L = 0.2$ mm the dimensionless scale l_T/δ_L becomes ~ 200. This point is shown on the Borghi diagram (Fig. 12) as a circle with the label "11% H2". A simple analysis shows with an arrow that for more reactive gas compositions the flame state approaches the flamelet regime and thus the flame has a potential to accelerate upstream the jet flow. On the other hand for less reactive mixtures, the flame state is shifted deeper into the flame instability zone (another arrow in Fig. 12) where the flame can quench due to an effective turbulent mixing.

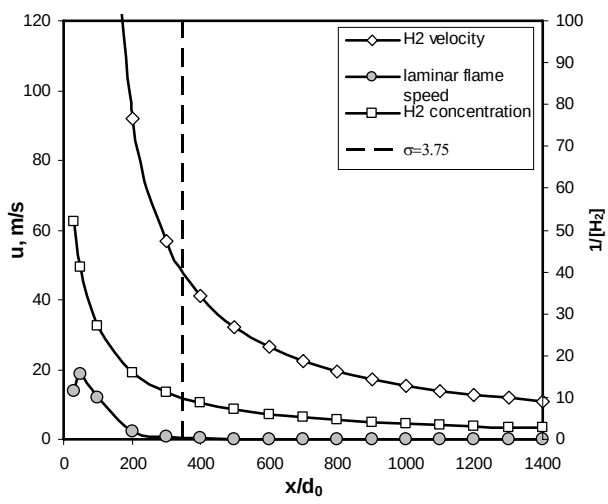

Figure 11. Main characteristics of hydrogen jet vs. distance from the nozzle

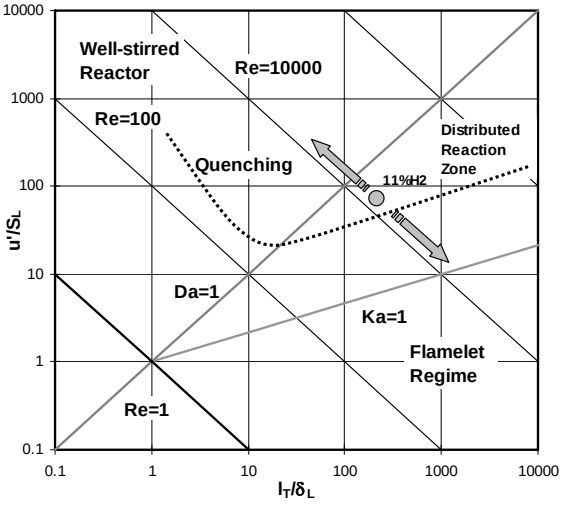

Figure 12. Borghi diagram for flame state at the critical ignition point

4.0 SUMMARY

Horizontal quasi-stationary high-momentum hydrogen jets with different nozzle diameters and different initial temperatures of 293K 80K and 35K have been investigated. An optical PIV method and sampling probe techniques combined with a gas analyzer have been used for jet structure investigation. It was shown that the experimental data are in good consistency with well known scale correlations [3]. Combustion experiments with variable ignition points showed that a stable flame with maximum flame velocity can only occur if the hydrogen concentration at the ignition point exceeds 11% of hydrogen. In this case the flame propagates up- and downstream of the jet, whereas in the opposite case the flame propagates only downstream or quenches.

ACKNOWLEDGEMENTS

This work was done within the Icefuel project (www.icefuel.de) which was funded by the German BMBF. Authors are very grateful to Mr. G. Markowz for technical support, supervision and useful suggestions throughout this research work.

REFERENCES

1. Dylla, A., H2-Transport durch Kabel. Energieversorgung „*HZwei – Das Magazin für Wasserstoff und Brennstoffzellen*“, 7. Jahrgang, April 2007
2. Schefer, R., Houf, W., San Marchi, C., Somerday, B., Keller, J., and Moen, C., Hydrogen Codes and Standards. Project Overview, Sandia National Laboratories, Livermore, CA, 11/3/2004
3. Chen, C. J., Rodi, W., Vertical turbulent buoyant jets: A review of experimental data. In: NASA STI/Recon Technical Report A 80, 1980
4. Dorofeev, S.B., Kuznetsov, M.S., Alekseev, V.I., Efimenko, A.A., Breitung, W., Evaluation of limits for effective flame acceleration in hydrogen mixtures. *Journal of Loss Prevention in the Process Industries*, **14**, No. 6, 2001, pp. 583-589
5. Klinge, F., Kirmse, T., Kompenhans, J., Application of Quantitative Background Oriented Schlieren (BOS) Proceedings of PSFVIP-4, June 3-5, 2003, Chamonix, France, paper F4097
6. Kähler, C., Sammler, B., Kompenhans, J., Generation and control of tracer particles for optical flow investigations in air. In: Experiments in Fluids, **33**, 2002, pp. 736–742